Available online at www.sciencedirect.com
SCIENCE DIRECT®
Journal of Chromatography A, 1006 (2003) 87–99
JOURNAL OF CHROMATOGRAPHY A
www.elsevier.com/locate/chroma

PowerFeed operation of simulated moving bed units: changing flow-rates during the switching interval

Ziyang Zhang[a], Marco Mazzotti[b], Massimo Morbidelli[a,*]

[a]*Swiss Federal Institute of Technology Zurich, Laboratorium für Technische Chemie/LTC, ETH-Hönggerberg/HCI, CH-8093 Zurich, Switzerland*

[b]*ETH Zürich, Institut für Verfahrenstechnik, Sonneggstrasse 3, CH-8092 Zurich, Switzerland*

Abstract

A possible way to improve the separation performance of simulated moving bed (SMB) units is to change the internal and external liquid flow-rates during the switching period. This operation mode, referred to as PowerFeed, is examined in this work through a model analysis. Similar to the Varicol process, which allows for the asynchronous movement of the ports, the PowerFeed process exhibits more degrees of freedom than the classical SMB process and therefore allows more room for optimization. Using an optimization technique based on a genetic algorithm, all three processes have been optimized for a few case studies in order to determine their relative potentials. It is found that PowerFeed and Varicol provide substantially equivalent performances, which are however significantly superior to those of the classical SMB process.

Keywords: Simulated moving bed chromatography; Varicol process; PowerFeed process; Optimization; Mathematical modelling; Enantiomer separation; Flow rates

1. Introduction

Simulated moving beds (SMBs) have been introduced [1] as a practical implementation of continuous countercurrent units, i.e., the so-called true moving beds (TMBs), in order to solve the problems associated with the movement of the solid. An SMB unit consists of a series of fixed bed columns connected in a circle and divided in four sections by two inlet ports (feed and eluent) and two outlet ports (raffinate and extract), as shown in Fig. 1. The countercurrent movement between the mobile phase and the stationary phase is simulated by synchronously moving the inlet and outlet ports in the same direction of the mobile phase flow. This unit, originally developed for the bulk separation of hydrocarbons, and subsequently extended to sugars, has been more recently applied to a wide range of separations and purifications, particularly in the pharmaceutical and fine chemical industries.

In order to make SMB units more efficient and competitive, several new operation modes have been introduced. These include supercritical fluid SMB [2–5], temperature gradient SMB [6], solvent gradient SMB [7–9] and multifraction SMB [10,11]. The first three improve the separation performance by properly changing the adsorption strength of the solute in the different sections of the unit. This is done by creating along the unit a gradient of pressure, temperature or solvent composition, respectively. Multifraction SMB units are based on the idea of increasing the number of purified fractions leaving

*Corresponding author. Tel.: +41-1-632-3034; fax: +41-1-632-1082.
E-mail address: morbidelli@tech.chem.ethz.ch (M. Morbidelli).

0021-9673/03/$ – see front matter
doi:10.1016/S0021-9673(03)00781-7

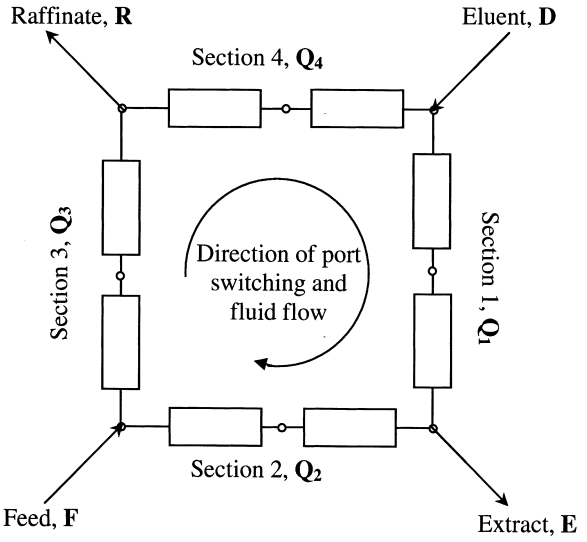

Fig. 1. Operating diagram of a four-section simulated moving bed (SMB) unit.

the unit by increasing the number of sections, that is, for example in the case of Nicolaos et al. [10,11] a five+four section unit for a three-component separation.

Another direction which has been taken to improve SMB performance is based on the idea of operating it under more complex forced dynamic conditions. In this context, the SMB unit is not regarded as an approximation (through appropriate discretization) of the TMB unit, but is regarded simply as a unit with many degrees of freedom that can be optimized to improve its performance. The first step in this direction is the Varicol unit [12,13], where the inlet and outlet ports are shifted asynchronously. This means that the unit is not any longer equivalent to a TMB, but that now it has some more parameters to be optimized, i.e., the switching times of the single inlet and outlet streams. A second possibility has been proposed originally in a patent [14] and more recently by Kloppenburg and Gilles [15] and Zang and Wankat [16], by considering fluid flow-rates changing in time during the switching period. In some sense these two processes can be traced back to a common origin, in that they force a time change during the switching period in either the solid or the fluid flow-rates, which are typically considered constant in TMB units and in the corresponding equivalent SMB units.

In this work, the possibility of changing the fluid flow-rates within the switching period, which we refer to in the following as ''PowerFeed'' operation, is investigated in detail, using multiobjective optimization technique. The optimal performances that can be achieved by the PowerFeed operation are compared with the corresponding ones given by Varicol and the classical SMB. The aim is to provide a clear picture, although inevitably confined to the cases examined, of the relative potential of these three operation modes.

As mentioned above, in the classical operation mode of the four-section SMB shown in Fig. 1, all the inlet (F and D), outlets (R and E) and internal flow-rates (Q_1–Q_4) are kept constant, while in the PowerFeed operation mode they change in time during the switching period. Actually, since only four of them are independent, in the following we force at most four flow-rates (Q_1, Q_2, F and D) to vary in time, while the other four follow from the mass balance ($Q_3=Q_2+F$, $Q_4=Q_1-D$, $R=Q_3-Q_4$, $E=Q_1-Q_2$). Although in principle these changes can be continuous in time, in this work, for computational convenience, we consider discontinuous changes, i.e., we assume that each flow-rate can change S times in a switching period t_s, each time taking a constant value. An example of PowerFeed operation is illustrated by the scheme in Fig. 2, where Q_1 is kept constant while Q_2, D and F are forced to take different values in three subintervals of the switching period t_s. As a consequence, E, Q_3, R and Q_4 also change three times in each switching interval.

2. Modeling and optimization of SMB, Varicol and PowerFeed processes

The same stage-in-series model described by Zhang et al. [17] has been adopted to simulate the SMB, Varicol and PowerFeed processeses, with a slight obvious revision, which enables the column flow-rates to change in time.

The separation problem taken as a case study requires the simultaneous maximization of the raffinate (P_R) and the extract purity (P_E) for a given feed, F, and eluent, D flow-rate, and a fixed configuration of the unit. In addition, in order to guarantee the same stationary phase and column mechanical

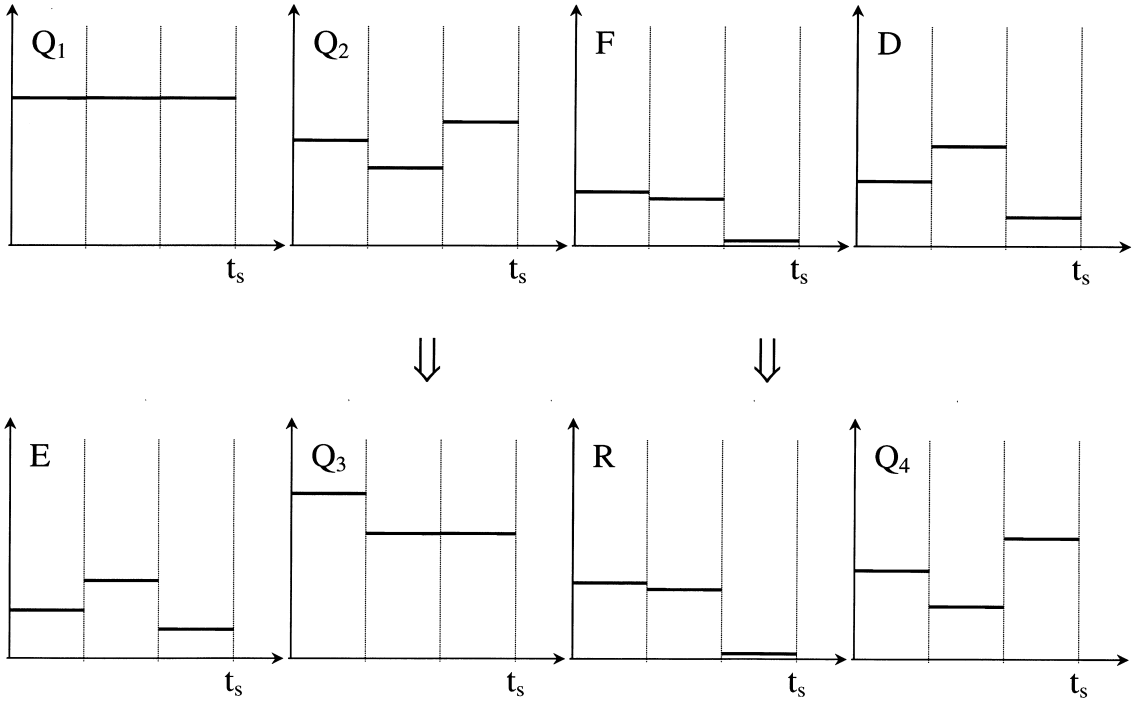

Fig. 2. An example of PowerFeed flow-rate variation scheme in three subintervals ($S=3$) during one switching period t_s.

characteristics we enforce the same pressure drop in all processes, which is done by fixing the flow-rate in Section 1, Q_1. This allows comparison of the three processes for fixed capital and operation costs (i.e., number and length of columns, amount of stationary phase and eluent consumption) and productivity. This optimization problem in the case of PowerFeed operation can be represented mathematically as follows:

$$\text{Max } J_1 = P_R \cdot [Q_{2,1}, \cdots, Q_{2,S}, F_1, \cdots, F_{S-1}, D_1, \cdots, D_{S-1}, t_s, \chi] \quad (1a)$$

$$\text{Max } J_2 = P_E \cdot [Q_{2,1}, \cdots, Q_{2,S}, F_1, \cdots, F_{S-1}, D_1, \cdots, D_{S-1}, t_s, \chi] \quad (1b)$$

subject to:

$$P_R \geq 90\% \quad (1c)$$

$$P_E \geq 90\% \quad (1d)$$

$$\text{Fixed values of } Q_1, F_{ave}, D_{ave}, N_{col}, N_{NTP} \quad (1e)$$

where N_{NTP}, i.e., the number of theoretical plates, defines the column efficiency, while $Q_{2,i}$, F_i and D_i represent the flow-rate in Section 2, the feed flow-rate and the eluent flow-rate in the ith subinterval of the switching period, respectively. It is worth noting that according to the above statement of the problem, the average feed and eluent flow-rates (F_{ave} and D_{ave}, respectively) are fixed, which is expressed in Eqs. (1a) and (1b) by the fact that the flow-rate in the last subinterval does not appear as an optimization variable. The column configuration is represented by the discrete variable χ, which can attain the values reported in Table 1 for five and six column units. It is to be noted that in the problem above the classical SMB operation mode has three decision variables, i.e., Q_2, t_s and χ. For the Varicol operation the decision variables are the same, but χ can attain a much larger number of values. In particular, in the SMB operation χ can attain only the values corresponding to the configurations reported in Table 1, which depend upon the total number of columns, N_{col}. In the Varicol process instead the number of

Table 1
Possible column configurations (distribution) for $N_{col}=5$ and $N_{col}=6$

χ	Column configuration[#]	χ	Column configuration
$N_{col}=5$			
A	2/1/1/1	C	1/1/2/1
B	1/2/1/1	D	1/1/1/2
$N_{col}=6$			
A	1/1/2/2	F	2/2/1/1
B	1/2/1/2	G	3/1/1/1
C	1/2/2/1	H	1/3/1/1
D	2/1/1/2	I	1/1/3/1
E	2/1/2/1	J	1/1/1/3

[#] Column distribution 2/1/1/1 implies two columns in section 1 and one column in sections 2–4.

possible configurations is determined by the number of subswitches considered in each switching interval, since in each of them the unit can take any of the configuration listed in Table 1, with the only constraint of periodicity, that is that the unit at the end of the switching period has to go back to the initial configuration. Thus for example, the complete configuration of a four-subinterval Varicol unit with $N_{col}=5$ can be described by the sequence A–B–C–D, which means that in the first quarter of the switching interval the unit has configuration 2/1/1/1, followed by configurations 1/2/1/1 and 1/1/2/1 in the second and third quarter, and finally 1/1/1/2 in the last one. This corresponds to a number of values accessible for χ equal to 16 for $N_{col}=5$ and 40 for $N_{col}=6$ in a four-subinterval unit.

For the PowerFeed operation mode the number of decision variables depends upon the number of subintervals (S) in which the switching interval has been divided, as indicated in Eqs. (1a) and (1b). Note that in this case it has been assumed that the flow-rates Q_2, F, D and consequently Q_3, Q_4, R and E, change in S subintervals, as illustrated in Fig. 2 for $S=3$. The problem can be simplified by changing in time a small number of flow streams, e.g., only F, which implies that also Q_3 and R change. In all cases the optimization problem has been solved using a rigorous multiobjective optimization technique, the non-dominated sorting genetic algorithm (NSGA), which has been proven to be efficient in optimizing SMB, Varicol [17] and SMB reactor processes [18].

3. Results and discussion

3.1. Nonlinear system

The first separation problem used in this work is the same chiral separation reported by Ludemann-Hombourger et al. [12], which has been examined earlier in the context of SMB and Varicol processes [17] and is described by the following modified Langmuir isotherm:

$$q_A = 2.63c_A + \frac{1.35c_A}{1 + 0.0647c_B + 0.04655c_A} \quad (2a)$$

$$q_B = 2.2c_B + \frac{1.23c_B}{1 + 0.0647c_B + 0.04655c_A} \quad (2b)$$

3.1.1. PowerFeed process where only F changes

In the first five-column PowerFeed configuration investigated, only the feed flow-rate, F changes in four subintervals ($S=4$). In this simplified case, the decision variables in Eqs. (1a) and (1b) reduce to Q_2, F_1, F_2, F_3, t_s and χ. The other parameter values are listed in Fig. 3, where the optimization results of the PowerFeed process are compared with those reported earlier [17] for the five-column SMB, six-column SMB and five-column Varicol processes. It is worth noting that, in all cases, we obtained a Pareto curve, i.e., a collection of optimal operating points such that when one moves from one to another one objective function improves but the other worsens, i.e., one purity increases and the other decreases. Each Pareto has at least one discontinuity due to a change in the optimal column configuration χ, given in the case of the PowerFeed operation by the line AB with the column configuration parameter $\chi=$B for high extract purities and line BC with $\chi=$C for high raffinate purities. This corresponds to the fact that in a five-column unit the fifth column should be located in Section 2, i.e., $\chi=$B when high-extract purities are required and in Section 3 or $\chi=$C when high-raffinate purities are required.

In Fig. 3 it is seen that the five-column PowerFeed process with the feed flow-rate, F varying in four subintervals improves the product purities over the corresponding SMB unit to an extent comparable to the four-subinterval Varicol unit. It should be noted that the comparison is done for the same average feed (F_{ave}) and eluent (D) flow-rates. The decision

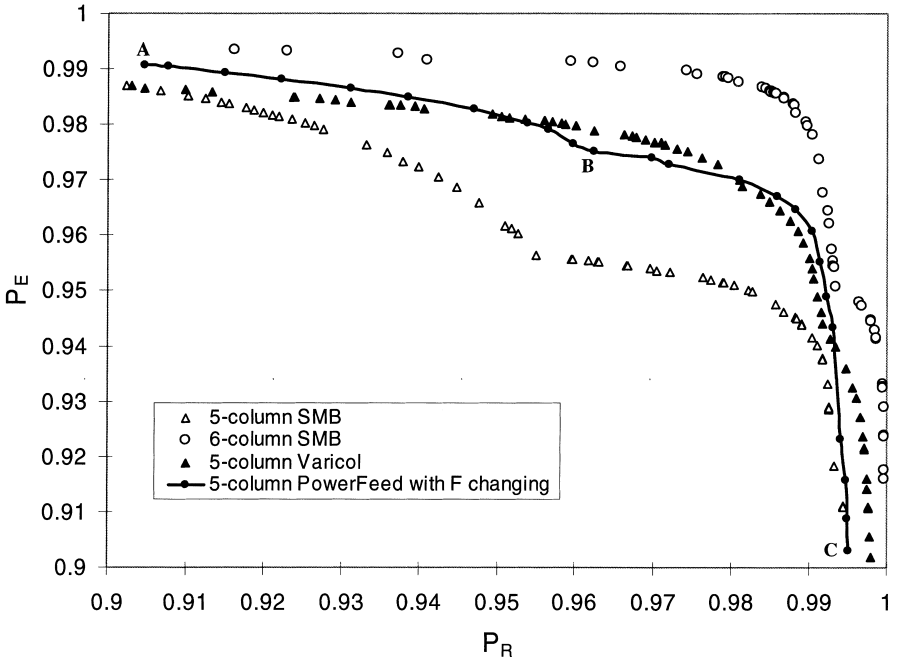

Fig. 3. Pareto sets for five-column SMB, six-column SMB, five-column Varicol with four subintervals and five-column PowerFeed with F changing in four subintervals. $Q_1 = 27.5$ ml/min, $F_{ave} = 1.62$ ml/min, $D = 6.24$ ml/min, $N_{col} = 5$, $N_{NTP} = 80$. Line AB: $\chi = B$ and line BC: $\chi = C$ for the five-column PowerFeed. The column configuration parameter χ changes from B to C, from C to E and from C–C–B–B to C–C–C–B to C–C–C–A with increasing P_R for the five-column SMB, six-column SMB and five-column Varicol processes, respectively.

variables, Q_2 and t_s, leading to optimal separation performance for the five-column PowerFeed process are compared with those of the five-column SMB process in Fig. 4a and b, respectively, showing that the two processes exhibit similar optimal values for these two operating variables. It is the feed variation in Fig. 4c (where F_4 is calculated from F_{ave} and the decision variables F_1, F_2 and F_3) that is responsible for the improved performance of the PowerFeed process. Note that the pattern of change of F in the PowerFeed operation changes as the column configuration χ changes. In the case of the configuration $\chi = B$, the highest feed flow-rate appears in the second and third subintervals and the lowest in the first, while where $\chi = C$, the feed streams in the first three subintervals are almost equal and such that there is almost no feed flow in the last one.

A better physical understanding of these results can be achieved by reasoning in terms of the flow-rate ratio parameters, m_j defined in the context of the equilibrium theory [19], as the ratio between the fluid and the solid flow-rates in each section of the unit. In Fig. 5a it is seen that the m values for the five-column SMB are almost constant, although m_2 and m_3 tend to decrease slightly as P_R increases. This is in agreement with triangle theory which, as discussed by Zhang et al. [17], indicates that the optimal operating conditions correspond to the vertex of the triangular complete separation region in the (m_2, m_3) plane. For the five-column PowerFeed process, the optimal m_3 values in each subinterval of the switching period are shown in Fig. 5b. It is interesting to note that the average m_3 values of the PowerFeed process, $m_{3,ave}$, are very close to the optimal m_3 values of the five-column SMB and Varicol processes, as shown in Fig. 5c. The slight difference in the optimal m_3 values between SMB and Varicol is due to the change in column configuration as discussed by Zhang et al. [17]. This indicates that all three processes, at least in average, adopt as optimal operating parameters the same flow-rate ratios, m_j, which, in the frame of equilibrium theory, correspond to the results of the triangle theory.

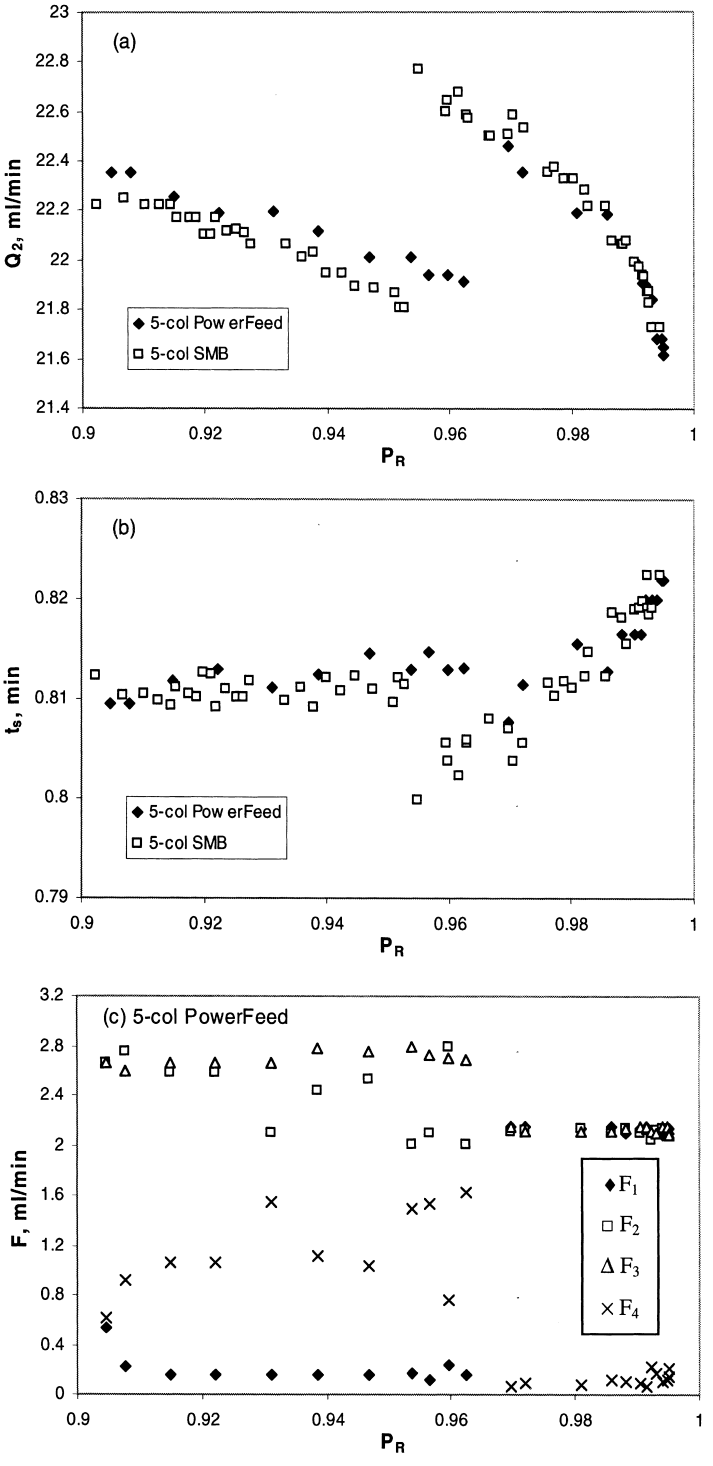

Fig. 4. Comparison of the decision variables corresponding to the optimal operating points on the Pareto sets of the five-column SMB and the five-column PowerFeed (line ABC) processes shown in Fig. 3.

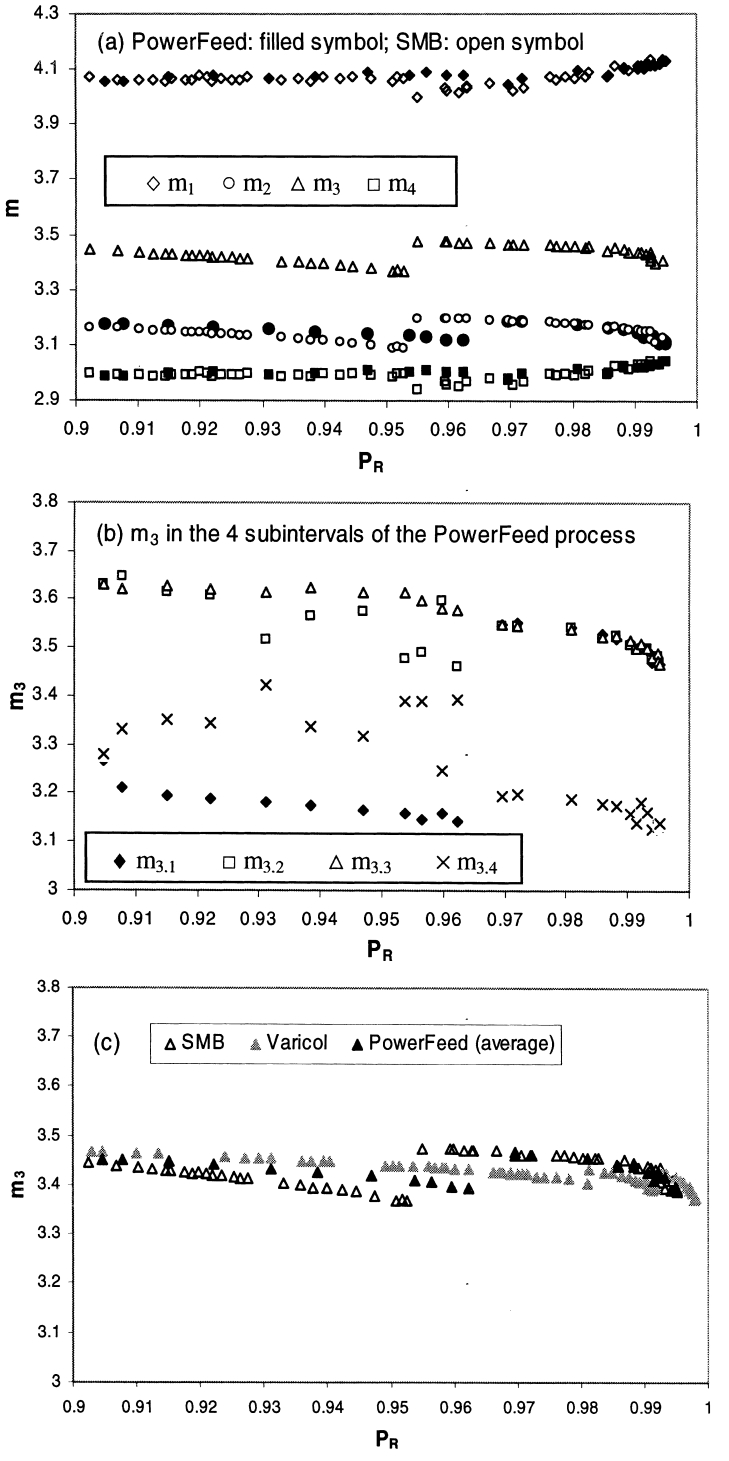

Fig. 5. Comparison of the optimal flow-rate ratio parameters corresponding to the points on the Pareto sets for the five-column SMB (open symbol) and the five-column PowerFeed (filled symbol) in Fig. 3. (a) Parameters m_1 to m_4 that do not change in the switching period; (b) optimal values of m_3 in the four subintervals of the five-column PowerFeed process; (c) optimal m_3 values for the SMB and Varicol processes and average optimal m_3 value for the PowerFeed process.

It is also interesting to note, by comparing Fig. 4a and b with Fig. 5a, that the calculated optimal values of the decision variables Q_2 and t_s are scattered, while those of the flow-rate ratio parameter m_2 (not a decision variable) follow a smooth line. This is a consequence of the fact that, as indicated by equilibrium theory, m_2 but not individually Q_2 and t_s control the unit performance. For this reason in the following we present the process optimal operating conditions only in terms of the flow-rate ratio parameters, m_j.

3.1.2. PowerFeed process where Q_2, F and D change

The above optimization problem has been repeated using a different PowerFeed configuration, where Q_2, F and D are changed in three subintervals ($S=3$) within the switching period. In this case, the decision variables in Eq. (1a) are nine: $Q_{2,1}$, $Q_{2,2}$, $Q_{2,3}$, F_1, F_2, D_1, D_2, t_s and χ. The optimization results are compared with those of the previous PowerFeed configuration where only the feed flow-rate was changed in four subintervals in Fig. 6. It is seen that the Pareto further improves, and actually becomes superior, although slightly, also of the five-column Varicol process. The optimal average flow-rate ratio parameters, m_{ave} of this PowerFeed process are compared to those of the five-column SMB process in Fig. 7a, while the m_2–m_4 values in each subinterval are shown in Fig. 7b–d. It is seen that also in this case the PowerFeed process acquires the same optimal operating conditions as the corresponding SMB process in terms of average flow-rate ratios, but its performance is better due to the change in time of operating conditions.

3.1.3. The case of a more difficult separation

As is often the case when introducing more degrees of freedom in a process, their impact is larger for more difficult operations. This is illustrated next by considering a more difficult separation process, that is the same chiral separation considered above but with an increased average feed flow-rate, F_{ave} from 1.62 to 2.2 ml/min, and a decreased column efficiency, N_{NTP} from 80 to 60. The five-column PowerFeed where Q_2, F and D are forced to

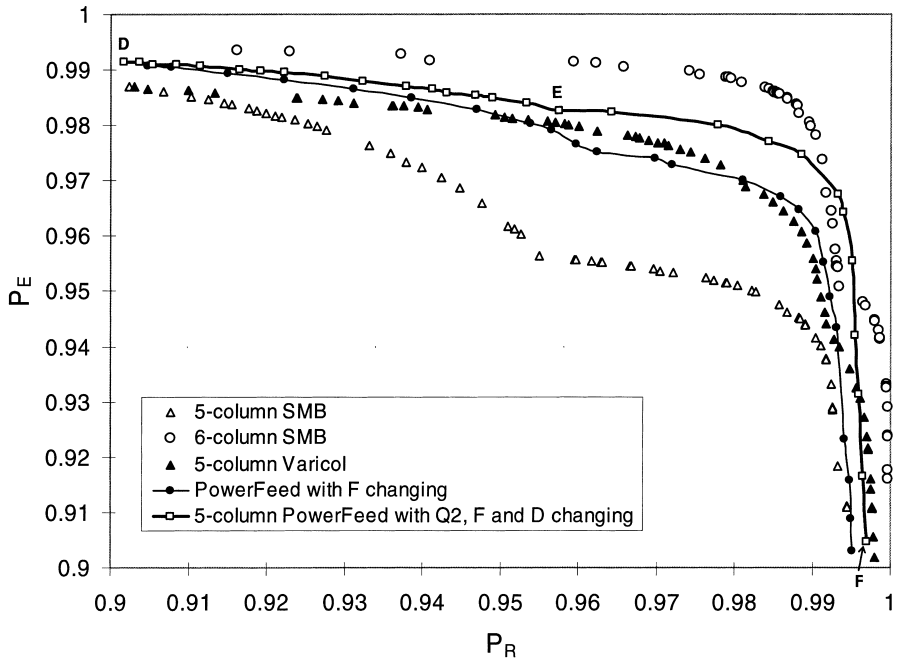

Fig. 6. Pareto set (line DEF) for the five-column PowerFeed process with Q_2, F and D changing in three subintervals ($S=3$). The other curves as in Fig. 3. $Q_1=27.5$ ml/min, $F_{ave}=1.62$ ml/min, $D_{ave}=6.24$ ml/min, $N_{col}=5$, $N_{NTP}=80$. Line DE: $\chi=$B; line EF: $\chi=$C.

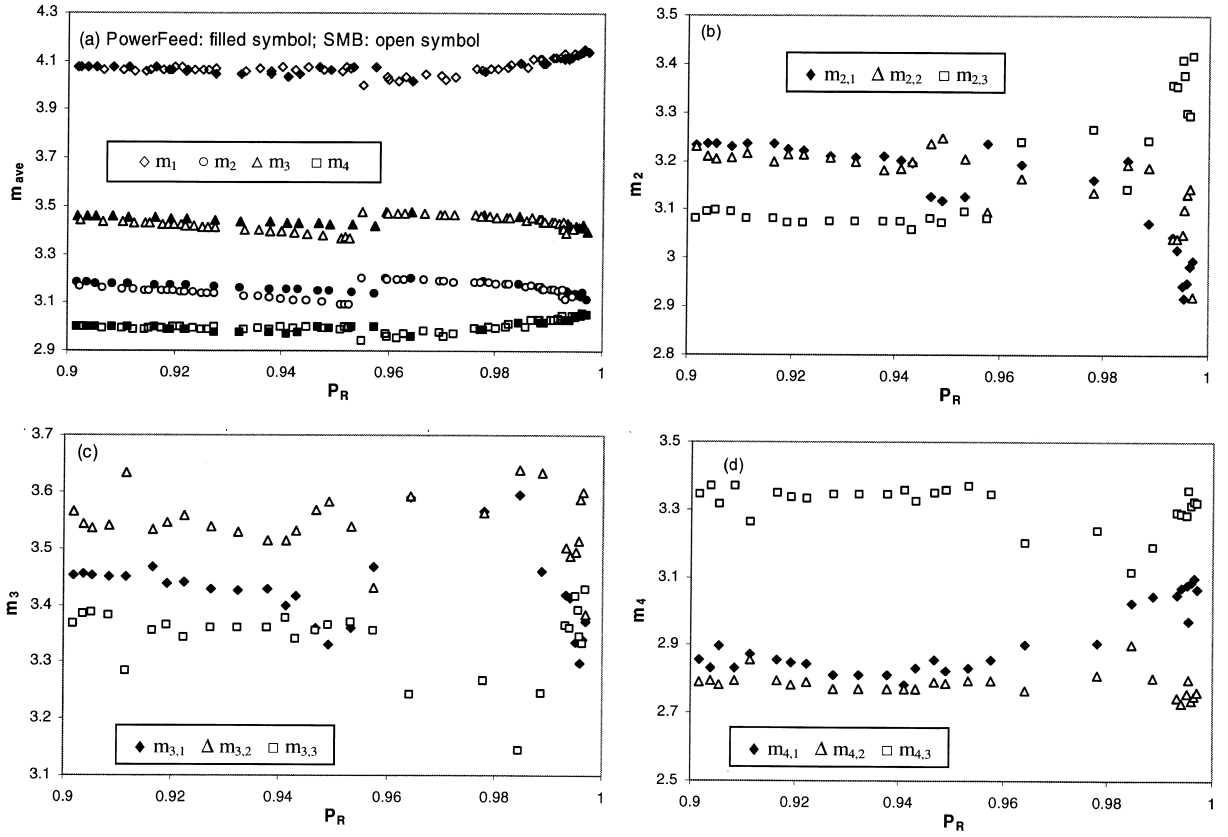

Fig. 7. (a) Comparison of the optimal m_{ave} values corresponding to the points on the Pareto sets of the five-column SMB (open symbol) and the PowerFeed (filled symbol) processes shown in Fig. 6; (b)–(d) optimal values of m_2 to m_4 in the three subintervals of the PowerFeed process (line DEF in Fig. 6).

change in time and the corresponding five-column SMB, five-column three-subinterval Varicol and six-column SMB processes have been optimized again according to Eq. (1a), and the corresponding optimal Pareto sets are compared in Fig. 8. It can be observed that the five-column PowerFeed performs better than the equivalent SMB and Varicol processes, and is even comparable to the six-column SMB for extreme purity specifications. By comparison with the results shown in Fig. 6 it is seen that the improvement provided by PowerFeed and Varicol over the classical SMB operation is larger when the separation is more difficult. The m_j values leading to optimal performances are shown in Fig. 9. Again, when considering average parameter values the optimal m_{ave} values of the PowerFeed process are the same as those for the classical SMB and for the Varicol processes.

3.2. The case of a linear separation

As a final example, the separation of α-ionone enantiomers [20] is considered. In this case, since the adsorption isotherm of the two enantiomers is linear, the model nonlinearity is strongly diminished but yet both Varicol and PowerFeed exhibit better performances. This result allows to better understand the physical nature of these process optimizations. All the relevant parameter values, including the Henry constants, column efficiency, hydrodynamics etc., have been taken from Zenoni et al. [20] considering the case where a mobile phase constituted by a

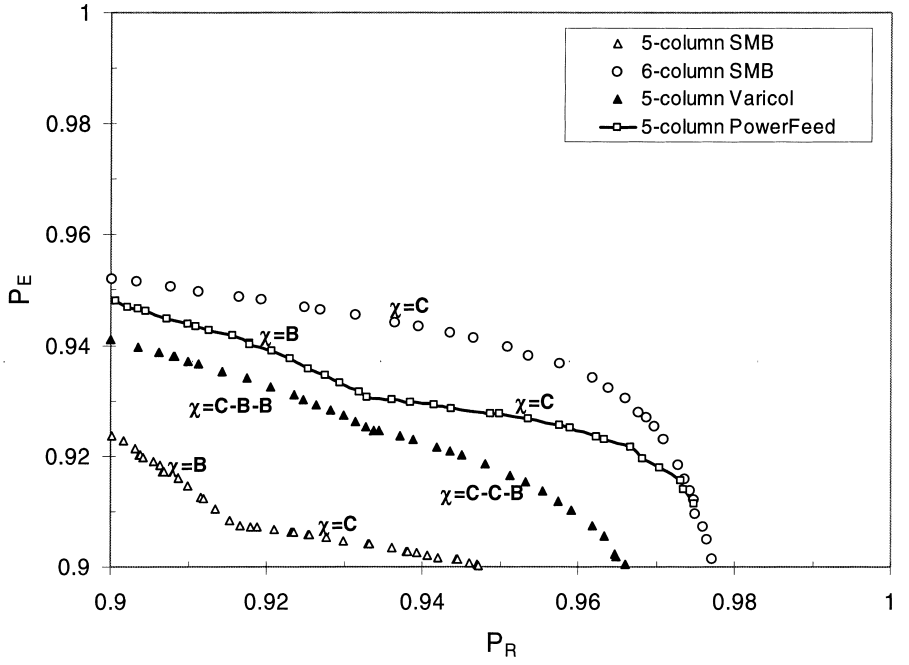

Fig. 8. Pareto sets for five-column SMB, six-column SMB, five-column Varicol with three subintervals and five-column PowerFeed with three subintervals ($S=3$) and changing Q_2, F and D. $Q_1=27.5$ ml/min, $F_{ave}=2.2$ ml/min, $D_{ave}=6.24$ ml/min, $N_{col}=5$ or 6, $N_{NTP}=60$.

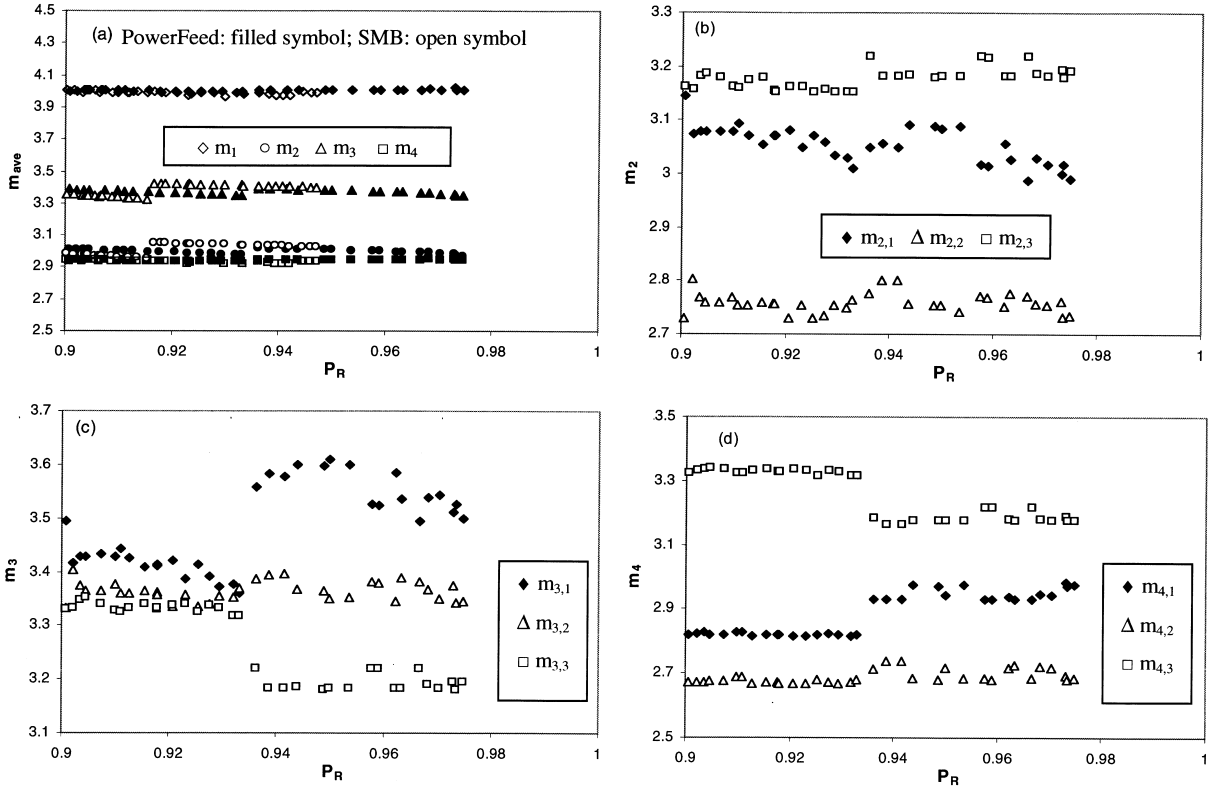

Fig. 9. (a) Comparison of the optimal m_{ave} values corresponding to the points on the Pareto sets of the five-column SMB (open symbol) and the five-column PowerFeed (filled symbol) processes shown in Fig. 8; (b)–(d) optimal values of m_2 to m_4 in the three subintervals of the PowerFeed process in Fig. 8.

methanol–water (70:30, v/v) mixture, and a temperature of $T=10$ °C have been used. The total feed concentration is fixed at 5 g/l.

Both purities in the extract and in the raffinate have been maximized, according to Eq. (1a), using a five-column PowerFeed process with three subintervals and changing Q_2, F and D, a classical five-column SMB process and a five-column Varicol process with four subintervals. The obtained Pareto curves are shown in Fig. 10, where the values of the operating parameters and the optimal column configurations are also reported. It is seen that, like in the cases of nonlinear separations, the PowerFeed process performs better than the SMB and similar to the Varicol process. The optimal operating conditions, in terms of average flow-rate ratio parameters, m_{ave}, are again the same for the three processes, as shown in Fig. 11a. The optimal values of the m_j parameters in the three subintervals are shown in Fig. 11b–d. From these results, it can be concluded that the performance improvement that can be achieved by forcing the dynamics of these processes is not due to their nonlinear behavior, but it is directly related to the nature of the process as discussed in the next section.

4. Concluding remarks

In this work we have considered four separation problems, involving both linear and nonlinear adsorption isotherms, and for each of them we have optimized and compared the SMB, the Varicol and the PowerFeed processes. The results show that the PowerFeed and the Varicol processes provide always significantly improved performances with respect to SMB, and that the extent of the improvement is larger for more difficult separations. This is due to the increased complexity of these two operation modes, which in essence allows to change during the switching period the solid or the fluid flow-rates inside the unit in order to improve the separation performance. In the reported examples some simple forms of such variations have been considered, thus

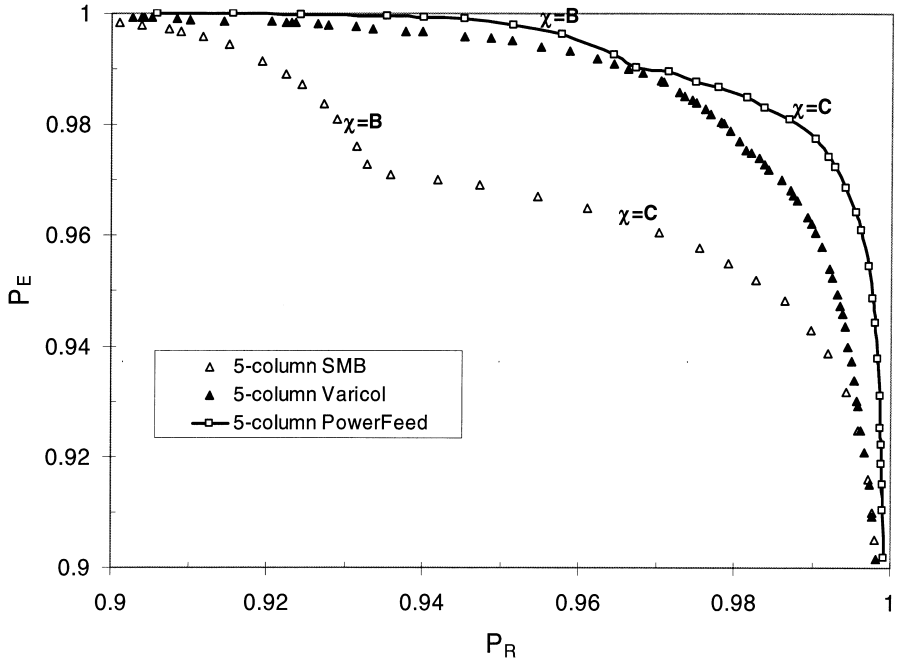

Fig. 10. Pareto sets for five-column SMB, five-column Varicol with four subintervals and five-column PowerFeed with three subinterval ($S=3$) and changing Q_2, F and D. $Q_1=4$ ml/min, $F_{ave}=0.9$ ml/min, $D_{ave}=2.2$ ml/min, $N_{col}=5$, $N_{NTP}=40$. The optimal column configuration for the five-column four-subinterval Varicol process changes along the Pareto curve from C–B–B–B to C–C–B–B to C–C–C–B to C–C–C–C as P_R increases.

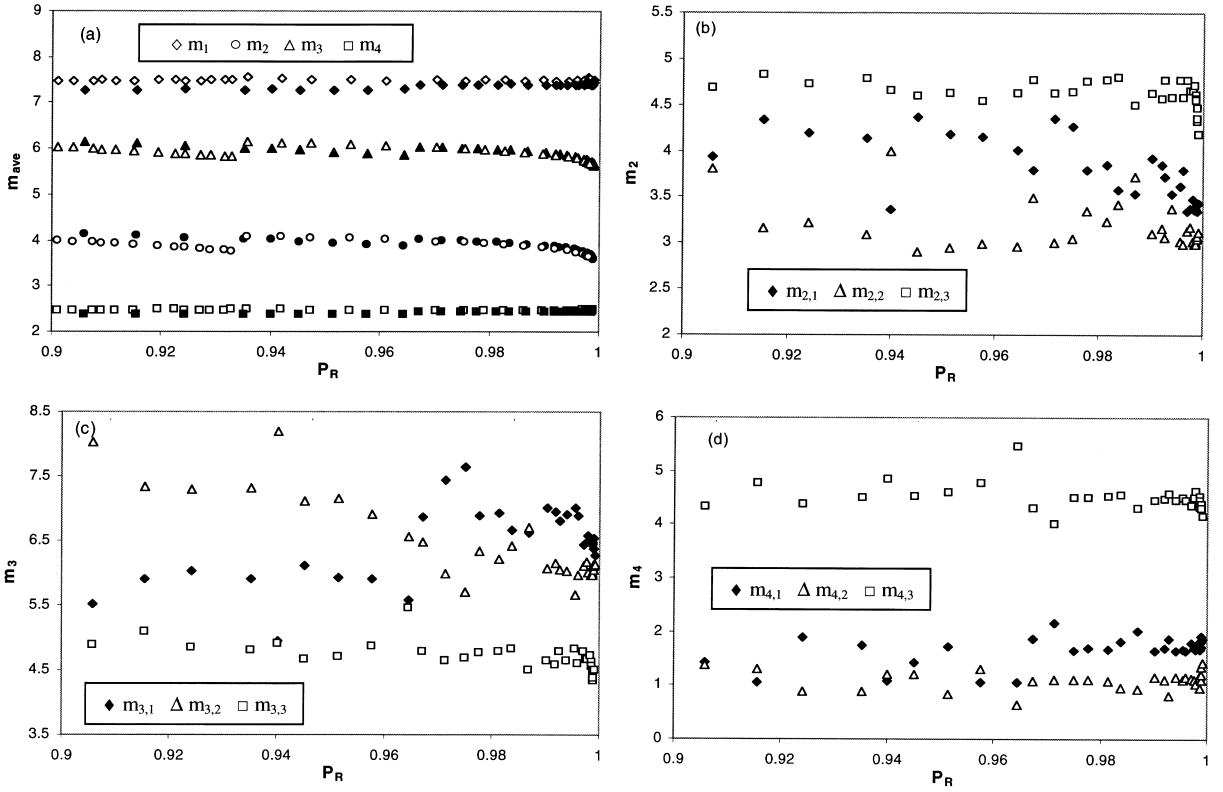

Fig. 11. (a) Comparison of the optimal m_{ave} values corresponding to the points on the Pareto sets of the five-column SMB (open symbol) and the five-column PowerFeed (filled symbol) processes shown in Fig. 10; (b)–(d) optimal values of m_2–m_4 in the three subintervals of the PowerFeed process in Fig. 10.

keeping relatively low the number of subintervals both in the Varicol and in the PowerFeed. This is not only due to the need of keeping relatively simple such operations in view of their practical implementation, but also because further subdivisions of the switching period bring to only marginal further improvements. A rigorous comparison between the two processes in general terms is not possible, but it is fair to say that they are equivalent in terms of potential performances, although Varicol is probably simpler to be implemented in practice than PowerFeed, since it does not require variation of flow-rates during a switching period. It is worth underlining that we have verified experimentally that PowerFeed operation is indeed feasible and effectively (Zhang et al., unpublished research).

An important result, which has been found in all examined cases, is that, when considering time averages, the values of the flow-rate ratio parameters, m_j, which lead to optimal operation of the three processes are very similar, although the separation performance achieved by each of them is different. This implies that, in the frame of equilibrium theory, the results of the triangle theory can be used to estimate the optimal operating flow-rate ratio parameters for each of these processes, at least in average terms.

On the other hand, the detailed optimization of these processes is not easy and genetic algorithms have been proved in this work to be rather effective with respect to alternative techniques [15]. Unfortunately, this numerical optimization has to be repeated for each separation problem under examination since for the PowerFeed process no general pattern has been found on how to change the flow-rates during the switching interval. One general observation, originally reported by Kloppenburg and Gilles [15] is that since as shown in Fig. 12 the pollutant in the extract is larger at the beginning of the switching period while that in the raffinate is

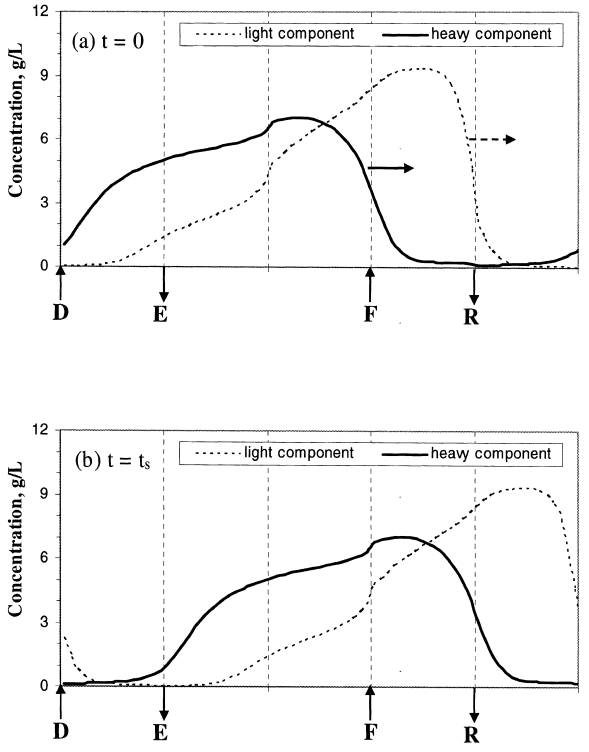

Fig. 12. Typical concentration profiles in a five-column SMB unit.

larger at the end, one should increase the extract flow-rate and decrease the raffinate flow-rate during the switching period. This concept, which applies equally well for linear and nonlinear systems, is probably too simplistic and in fact the optimal flow-rates computed in the cases reported above do not exhibit this pattern of behavior.

5. Nomenclature

c	Liquid phase concentration (g/l)
D	Eluent flow-rate (ml/min)
E	Flow-rate of extract stream (ml/min)
F	Feed flow-rate (ml/min)
H_i	Henry constant of component i
J	Objective function
m	Flow-rate ratio parameter
N_{col}	Total number of columns
N_{NTP}	Number of theoretical plates
P_E	Purity of extract stream (%)
P_R	Purity of raffinate stream (%)
q	Solid-phase concentration (g/l)
Q_j	Fluid flow-rate in section j (ml/min)
R	Flow-rate of raffinate stream (ml/min)
S	Number of subintervals
t_s	Switching time (min)

Symbols

χ	Column configuration

Subscripts and superscripts

ave	Average
A	Strongly adsorbed component
B	Weakly adsorbed component
j	Section j
S	Subinterval S

References

[1] D.B. Broughton, C.G. Gerhold, US Pat. 2 985 589 (1961).
[2] R.M. Nicoud, M. Perrut, Fr. Pat. 9 205 304 (1992).
[3] M. Mazzotti, G. Storti, M. Morbidelli, J. Chromatogr. A 786 (1997) 309.
[4] O. Di Giovanni, M. Mazzotti, M. Morbidelli, F. Denet, W. Hauck, R.M. Nicoud, J. Chromatogr. A 919 (2001) 1.
[5] F. Denet, W. Hauck, R.M. Nicoud, O. Di Giovanni, M. Mazzotti, J.N. Jaubert, M. Morbidelli, Ind. Eng. Chem. Res. 40 (2001) 4603.
[6] C. Migliorini, M. Wendlinger, M. Mazzotti, M. Morbidelli, Ind. Eng. Chem. Res. 40 (2001) 2606.
[7] T.B. Jensen, T.G.P. Reijns, H.A.H. Billiet, L.A.M. van der Wielen, J. Chromatogr. A 873 (2000) 149.
[8] D. Antos, A. Seidel-Morgenstern, Chem. Eng. Sci. 56 (2001) 6667.
[9] S. Abel, M. Mazzotti, M. Morbidelli, J. Chromatogr. A 944 (2002) 23.
[10] A. Nicolaos, L. Muhr, P. Gotteland, R.M. Nicoud, M. Bailly, J. Chromatogr. A 908 (2001) 71.
[11] A. Nicolaos, L. Muhr, P. Gotteland, R.M. Nicoud, M. Bailly, J. Chromatogr. A 908 (2001) 87.
[12] O. Ludemann-Hombourger, R.M. Nicoud, M. Bailly, Sep. Sci. Technol. 35 (2000) 1829.
[13] O. Ludemann-Hombourger, G. Pigorini, R.M. Nicoud, D.S. Ross, G. Terfloth, J. Chromatogr. A 947 (2002) 59.
[14] M.M. Kearney, K.L. Hieb, US Pat. 5 102 553 (1992).
[15] E. Kloppenburg, E.D. Gilles, Chem. Eng. Technol. 22 (1999) 813.
[16] Y. Zang, P.C. Wankat, Ind. Eng. Chem. Res. 41 (2002) 2504.
[17] Z. Zhang, K. Hidajat, A.K. Ray, M. Morbidelli, AIChE J. 48 (2002) 2800.
[18] Z. Zhang, K. Hidajat, A.K. Ray, Ind. Eng. Chem. Res. 41 (2002) 3213.
[19] M. Mazzotti, G. Storti, M. Morbidelli, J. Chromatogr. A 769 (1997) 3.
[20] G. Zenoni, F. Quattrini, M. Mazzotti, C. Fuganti, M. Morbidelli, Flavour Frag. J. 17 (2002) 195.